Functional plasmonic nanoantennae as optical filters

Jiangtao Lv[1], *Hailong Liu*[2], *Guangyuan Si*[1]

[1]*College of Information Science and Engineering, Northeastern University, Shenyang 110004, People's Republic of China*
[2]*Measurement Technology and Instrumentation Key Laboratory of Hebei Province, Yanshan University, Qinhuangdao 066004, People's Republic of China*
E-mail: siguang0323@hotmail.com

Published in Micro & Nano Letters; Received on 14th September 2014; Revised on 26th October 2014; Accepted on 10th November 2014

Plasmonic nanoantennae are important candidates for metamaterials in the visible range. However, the fabrication of dense nanoantennae with various designs and small dimensions is still very challenging for nanoscale features with high aspect ratios. Demonstrated is a series of geometries of plasmonic nanocrystals with different designs and ultrasmall gaps using a one-step focused ion beam milling process. Optical characterisation of plasmonic nanoantennae has also been carried out to investigate the underlying physics. Theoretical calculations were also performed to verify the experimental results. The high fabrication quality nanostructures demonstrated may enable new applications in nanophotonics, giving rise to new opportunities for nanodevices.

1. Introduction: Investigations on surface plasmons [1–3], which are electromagnetic oscillations existing at metallic–dielectric interfaces, have attracted increasing interest recently and paved the way for controlling optical signals at varying frequency bands because of their irreplaceable and unique properties. Plasmonics mainly benefits from the advance of nanotechnology, enabling various plasmon-based components or optical elements which can achieve super resolution [4–6], invisible cloaking [7–9], high-intensity lasing [10], active switching [11–13] and even computing [14]. Such devices are capable of tuning plasmon resonances to a great extent. Among all the applications mentioned above, the possibility of engineering various plasmonic nanostructures with ultrasmall dimensions has attracted increasing interest because of their special importance. More importantly, plasmonic nanoantennae with ultrasmall gaps enable considerable enhancement of the near-field intensity, leading to helpful applications in surface-enhanced Raman scattering detection [15–17] and microscopy. Antennae have the capability of transmitting and receiving information over a wide spectral range and converting confined energy into radiated waves. Owing to the powerful ability of generating intense electric fields, different optical nanoantennae can be applied to various frequencies [18–20]. The important applications of nanoantenna arrays also include lifetime controlling [21, 22] and beam-steering [23]. Nanoantennae also find applications for wavelength-selective photoswitches [24], sensors [25] and absorbers [26].

Plasmonic nanoantennae with ultrasmall inter-particle separations and high density are important candidates for optical components because they can generate an optical response in visible frequencies and furthermore lead to useful applications in photonics and integrated optics. Small gaps enable dramatically enhanced near-field intensity which is important for a broad scope of applications [27–29]. Such optical components take advantage of the novel properties of plasmonics which are barely available using any other traditional methods or dielectric structures.

The main obstruction for fabricating nanoantennae at higher frequencies are the well-known difficulties of processing metallic devices with ultrasmall dimensions. Thus, most plasmonic devices are normally fabricated using top-down methods such as lithography and direct milling, which can define well-aligned arrays with varying geometric parameters. Electron-beam lithography can define arbitrary geometries at nanoscales. It is frequently used with peeling-off or etching to transfer patterns from resists to different materials. Alternatively, one can directly pattern almost all kinds of desired structures on almost all kinds of materials via focused ion beam (FIB) milling. Equipped with a liquid ion source, FIB systems can drill, deposit, image and form small probe beams with high-current densities. New generations of FIB systems utilise helium ions instead of gallium to achieve smaller features with fine structural parameters [30–34] since helium ions are much lighter than gallium ions, enabling structures with ultrasmall dimensions. Here, we report on the fabrication of nanoantennae plasmonic crystals with desired outlines and ultrasmall gap widths using a novel approach based on one-step FIB lithography using gallium ions (FIB 200, FEI Company). We show that it is feasible to achieve fine features with ultrasmall gaps and high density by accurately controlling the milling variables. By overlapping proper patterns with tunable geometric parameters, a variety of designs are achieved, including satellite-surrounded particles and diamond-shaped nanoclusters. Moreover, optical filters are demonstrated using varying arrays, which show great potential for applications in designing optical devices. To verify the experimental results, finite-difference time-domain (FDTD) simulations were also performed and reasonable agreement is shown. The elegant approach achieved here may find new opportunities for nanophotonics and optics.

2. Fabrication: Quartz substrates (refractive index $n = 1.46$) were first cleaned and then loaded in an electron-beam evaporator for metal film deposition. The pressure of the chamber was stabilised at 4×10^{-7} mbar. Then 4 nm titanium and 110 nm gold were subsequently deposited onto the sample surface. All patterns were milled in parallel to avoid materials redeposition using a single-beam equipment. The probe current 11 pA was selected with 30 kV acceleration voltage. Note that not only the parameters of the patterns but also milling time is extremely important since even tiny overmilling can severely damage the surface of a sample and affect the final outlines and sidewall profiles of the fabricated devices. Ions can directly bombard materials with high density, enabling direct pattern transfer to different substrates. However, the collision between heavy ions and atoms of materials under consideration makes it possible to fabricate high aspect ratio structures and narrow line widths.

3. Results and discussion: Fig. 1 shows the scanning electron microscope (SEM) images of four designs under investigation in this work. Fig. 1*a* shows centred particles surrounded by four

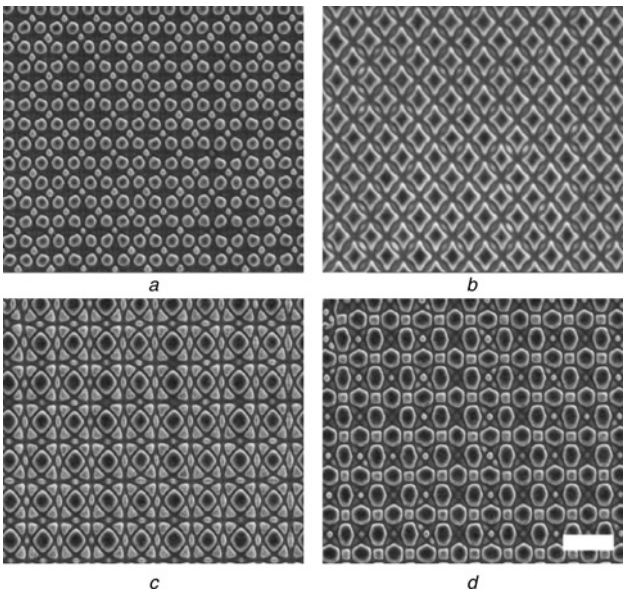

Figure 1 *SEM images of four typical designs under investigation in this work. Scale bar, 1 μm*
a Centred particles surrounded by four round satellites
b Diamond-shaped clusters
c Diamond-shaped centre particles surrounded by satellite triangles
d Square-shaped centre particles surrounded by hexagon satellites

round satellites and Fig. 1*b* demonstrates diamond-shaped clusters. Figs. 1*c* and *d* show diamond-shaped centre particles surrounded by satellite triangles and square-shaped centre particles surrounded by hexagon satellites, respectively. By design, one can readily fabricate various nanodevices with similar architectures. Strong contrast at the boundary of the particles is because of materials redeposition effects. It is worth noting that the milling-induced damage is serious if the milling time is increased, leading to rough surfaces and depressed device performance. Therefore, one needs to select an appropriate probe current to balance the total milling time and device profile.

The measured transmission of Figs. 1*a* and *b* are plotted in Fig. 2*a*. The optical filter function can be achieved using different designs, as clearly demonstrated. The filter effect ranges from 500 to 700 nm and 1000 to 1300 nm, respectively. Note that a micro-spectrometer (QDI 2010^{TM}, CRAIC Technologies) with a 75 W xenon source was used to perform the characterisation of the fabricated devices at normal incidence. The transmitted intensity was normalised to the light through a bare substrate without patterns. The measured transmittance of the structures in Figs. 1*c* and *d* is plotted in Fig. 2*b*. The filter effect ranges from 400 to 650 nm and 900 to 1300 nm, respectively. The interaction between neighbouring nanoantennae changes from the weak coupling regime to the strong coupling regime with decreasing gap width. Considerably enhanced field enhancement leads to useful optical properties which can find extensive important applications in a broad area of research. When the wavelength of the incident light is fixed, the interaction term accumulates phase delays during propagating between the antennae with increasing lattice separations. Additionally, large scattering may be caused by rough surfaces and sidewalls as well as grain boundaries after fabrication. Clearly, there are two peaks that can be observed for the red curve in Fig. 2*b* in the band of 400–600 nm, locating at ~480 and 550 nm, respectively.

To further verify the measurements, FDTD calculations (Lumerical) were carried out. During simulations, the mesh size was fixed as 5 nm × 5 nm × 5 nm. We calculated the corresponding transmittance spectra of the nanoantenna array in Figs. 1*b* and *c*.

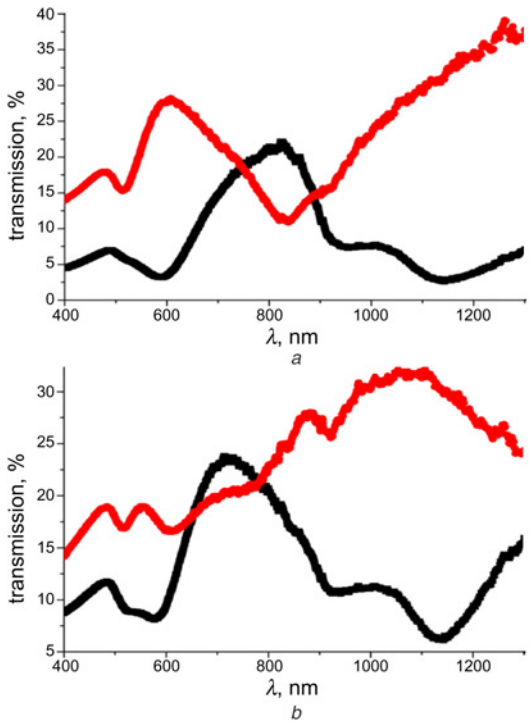

Figure 2 *Measured transmission for structures shown in Figs. 1a/b and c/d, respectively*
a Transmission spectra for structures shown in Figs. 1*a* (red curve) and *b* (black curve)
b Transmission spectra for structures shown in Figs. 1*c* (red curve) and *d* (black curve)

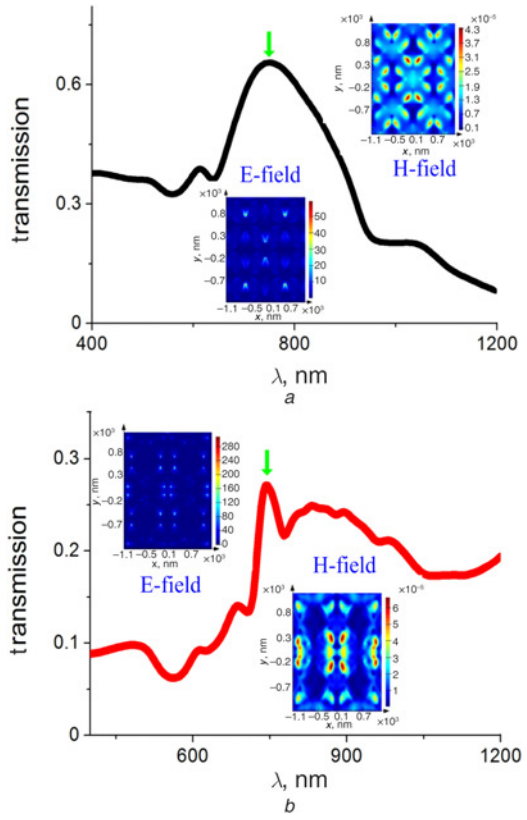

Figure 3 *Calculated transmission for structures shown in Figs. 1b and c*
a Structure of Fig. 1*b*
b Structure of Fig. 1*c*
Insets: Electric- and magnetic-field distributions corresponding to resonances (indicated by green arrows) of filters

doi: 10.1049/mnl.2014.0525

Overall, the simulated results agree well with the measured spectra. To further investigate the underlying physics of the filtering effects of these nanoantennae, the near-field electric- and magnetic-field distributions corresponding to the resonances of the filters (marked by green arrows in Fig. 3) were calculated and are shown in the insets of Fig. 3.

In Fig. 3*a*, the filter resonance frequency is because of the dipolar plasmon couplings between the opposite tips of the diamond antennae. The resonance peak marked by the green arrow in Fig. 3*b* is affected by the dipolar plasmon coupling between the four small particles. In addition to these small resonated particles, the big square nanoparticles also oscillate as antennae, and their coupling forms the broad peak about 900 nm in Fig. 3*b*. Therefore, different sizes and shapes of nanoparticles can be employed as nanoantennae and tuned to form band filters. The difference between experiments and calculations is mainly attributed to the convergence of numerical iterations. In addition, large scattering may be caused by rough surfaces and sidewalls as well as grain boundaries after fabrication, which is different from the ideal case in simulations. More importantly, both normal and oblique incident waves could be collected during measurements, while only normal incidence energy was detected during simulations. It is also worth noting that the fabrication imperfections may cause different charge distributions on the top of the nanoantennae, resulting in alterative optical properties in the transmission spectrum since the dipolar resonance of the centre antenna can be converted to a superradiant mode because of intense hybridisation with the plasmon modes of the surrounding satellite antennae. Therefore, the plasmon resonance may not be as pronounced when using objectives with inappropriate incidence angles or numerical apertures during the characterisation.

4. Conclusion: We have shown a new method to fabricate novel plasmonic nanoantenna structures of different designs. The optical properties were characterised and theoretical calculations were performed to verify the measured results. Reasonable agreement is achieved. Effective plasmon resonance tuning effects and different optical applications are realised. Desired features with varying structural parameters are enabled in noble metals, leading to useful devices which are extremely important for nanophotonics and integrated optics.

5. Acknowledgments: This work was supported by NEU internal funding (grant nos. XNB201302 and XNK201406), the Natural Science Foundation of Hebei Province (grant nos. A2013501049 and F2014501127), the Science and Technology Research Funds for Higher Education of Hebei Province (grant no. ZD20132011), the Fundamental Research Funds for the Central Universities (grant nos. N120323002 and N120323014), the Specialised Research Fund for the Doctoral Program of Higher Education (grant no. 20130042120048), the Science and Technology Foundation of Liaoning Province (grant no. 20131031) and the Scientific Research Foundation for the Returned Overseas Chinese Scholars, State Education Ministry (grant no. 47–4).

6 References

[1] Ebbesen T.W., Lezec H.J., Ghaemi H.F., Thio T., Wolff P.A.: 'Extraordinary optical transmission through sub-wavelength hole arrays', *Nature*, 1998, **391**, pp. 667–669
[2] Barnes W.L., Dereux A., Ebbesen T.W.: 'Surface plasmon subwavelength optics', *Nature*, 2003, **424**, pp. 824–830
[3] Genet C., Ebbesen T.W.: 'Light in tiny holes', *Nature*, 2007, **445**, pp. 39–46
[4] Zhao Y., Gan D., Cui J., Wang C., Du C., Luo X.: 'Super resolution imaging by compensating oblique lens with metallodielectric films', *Opt. Express*, 2008, **16**, pp. 5697–5707
[5] Zhao Y., Nawaz A.A., Lin S.S., Hao Q., Kiraly B., Huang T.J.: 'Nanoscale super-resolution imaging via metal-dielectric metamaterial lens system', *J. Phys. D, Appl. Phys.*, 2011, **44**, (41), pp. 415101–415107
[6] Zhao Y., Lin S.S., Nawaz A.A., *ET AL.*: 'Beam bending via plasmonic lenses', *Opt. Express*, 2010, **18**, pp. 23458–23465
[7] Li J., Pendry J.B.: 'Hiding under the carpet: a new strategy for cloaking', *Phys. Rev. Lett.*, 2008, **101**, p. 23901
[8] Milton G.W., Briane M., Willis J.R.: 'On cloaking for elasticity and physical equations with a transformation invariant form', *New J. Phys.*, 2006, **8**, p. 248
[9] Cummer S.A., Schurig D.: 'One path to acoustic cloaking', *New J. Phys.*, 2007, **9**, p. 45
[10] Oulton R.F., Sorger V.J., Zentgraf T., *ET AL.*: 'Plasmon lasers at deep subwavelength scale', *Nature*, 2009, **461**, pp. 629–632
[11] Liu Y.J., Hao Q.Z., Smalley J.S.T., Liou J., Khoo I.C., Huang T.J.: 'A frequency-addressed plasmonic switch based on dual-frequency liquid crystals', *Appl. Phys. Lett.*, 2010, **97**, p. 091101
[12] Liu Y.J., Zheng Y.B., Liou J., Chiang I.K., Khoo I.C., Huang T.J.: 'All-optical modulation of localized surface plasmon coupling in a hybrid system composed of photo-switchable gratings and Au nanodisk arrays', *J. Phys. Chem. C*, 2011, **115**, pp. 7717–7722
[13] Liu Y.J., Zheng Y.B., Shi J., Huang H., Walker T.R., Huang T.J.: 'Optically switchable gratings based on azo-dye-doped, polymer-dispersed liquid crystals', *Opt. Lett.*, 2009, **34**, pp. 2351–2353
[14] Johnston M.M.W., Wilson D.M., Booksh K.S., Cramer J.: 'Integrated optical computing: system on chip for surface plasmon resonance imaging'. Proc. Int. Conf. on IEEE Int. Symp. on Circuits and Systems, Kobe, Japan, May 2005, Vol. 4, pp. 3483–3486
[15] Gu Y., Li H., Xu S., Liu Y., Xu W.: 'Evanescent field excited plasmonic nano-antenna for improving SERS signal', *Phys. Chem. Chem. Phys.*, 2013, **15**, (37), pp. 15494–15498
[16] Li W.D., Ding F., Hu J., Chou S.Y.: 'Three-dimensional cavity nanoantenna coupled plasmonic nanodots for ultrahigh and uniform surface-enhanced Raman scattering over large area', *Opt. Express*, 2011, **19**, pp. 3925–3936
[17] Li Z.Y., Hattori T.H., Parkinson P., *ET AL.*: 'A plasmonic staircase nano-antenna device with strong electric field enhancement for surface enhanced Raman scattering (SERS) applications', *J. Phys. D, Appl. Phys.*, 2012, **45**, p. 305102
[18] Krasnok A.E., Simovski C.R., Belov P.A., Kivshar Y.S.: 'Superdirective dielectric nanoantennas', *Nanoscale*, 2014, **6**, pp. 7354–7361
[19] Bonakdar A., Mohseni H.: 'Impact of optical antennas on active optoelectronic devices', *Nanoscale*, 2014, **6**, pp. 10961–10974
[20] Schäfer C., Gollmer D.A., Horrer A., *ET AL.*: 'A single particle plasmon resonance study of 3D conical nanoantennas', *Nanoscale*, 2013, **5**, pp. 7861–7866
[21] Bakker R.M., Drachev V.P., Liu Z.T., *ET AL.*: 'Nanoantenna array-induced fluorescence enhancement and reduced lifetimes', *New J. Phys.*, 2008, **10**, p. 125022
[22] Adato R., Yanik A.A., Wu C.H., Shvets G., Altug H.: 'Radiative engineering of plasmon lifetimes in embedded nanoantenna arrays', *Opt. Express*, 2010, **18**, pp. 4526–4537
[23] DeRose C.T., Kekatpure R.D., Trotter D.C., *ET AL.*: 'Electronically controlled optical beam-steering by an active phased array of metallic nanoantennas', *Opt. Express*, 2013, **21**, pp. 5198–5208
[24] Lin Y.K., Ting H.W., Wang C.Y., *ET AL.*: 'Au nanocrystal array/silicon nanoantennas as wavelength-selective photoswitches', *Nano Lett.*, 2013, **13**, (6), pp. 2723–2731
[25] Smythe E.J., Cubukcu E., Capasso F.: 'Optical properties of surface plasmon resonances of coupled metallic nanorods', *Opt. Express*, 2007, **15**, pp. 7439–7447
[26] Hao J.M., Wang J., Liu X.L., Padilla W.J., Zhou L., Qiu M.: 'High performance optical absorber based on a plasmonic metamaterial', *Appl. Phys. Lett.*, 2010, **96**, p. 251104
[27] Koh A.L., Tomanec O., Urbánek M., Šikola T., Maier S.A., McComb D.W.: 'HRTEM and EELS of nanoantenna structures fabricated using focused ion beam techniques', *J. Phys., Conf. Ser.*, 2010, **241**, p. 012041
[28] Novotny L., van Hulst N.: 'Antennas for light', *Nat. Photonics*, 2011, **5**, pp. 83–90
[29] Black L.J., Wang Y.D., de Groot C.H., Arbouet A., Muskens O.L.: 'Optimal polarization conversion in coupled dimer plasmonic nanoantennas for metasurfaces', *ACS Nano*, 2014, **8**, (6), pp. 6390–6399
[30] Kollmann H., Piao X., Esmann M., *ET AL.*: 'Toward plasmonics with nanometer precision: nonlinear optics of helium-ion milled gold nanoantennas', *Nano Lett.*, 2014, **14**, pp. 4778–4784
[31] Wang Y., Abb M., Boden S.A., Aizpurua J., de Groot C.H., Muskens O.L.: 'Ultrafine control of partially loaded single plasmonic

nanoantennas fabricated using e-beam lithography and helium ion beam milling'. Proc. CLEO: QELS_Fundamental Science, San Jose, CA, USA, 2014

[32] Scholder O., Jefimovs K., Shorubalko I., Hafner C., Sennhauser U., Bona G.L.: 'Helium focused ion beam fabricated plasmonic antennas with sub-5 nm gaps', *Nanotechnology*, 2013, **24**, (39), p. 395301

[33] Wang Y., Boden S.A., Bagnall D.M., Rutt H.N., de Groot C.H.: 'Helium ion beam milling to create a nano-structured domain wall magnetoresistance spin valve', *Nanotechnology*, 2012, **23**, (59), p. 395302

[34] Wang Y., Abb M., Boden S.A., Aizpurua J., de Groot C.H., Muskens O.L.: 'Ultrafast nonlinear control of progressively loaded, single plasmonic nanoantennas fabricated using helium ion milling', *Nano Lett.*, 2013, **13**, (11), pp. 5647–5653

doi: 10.1049/mnl.2014.0525